Experimental probe of adsorbate binding energies at internal crystalline/amorphous interfaces in Gd-doped Si_3N_4

Klaus van Benthem,[1,a)] Gayle S. Painter,[2] Frank W. Averill,[3] Stephen J. Pennycook,[2] and Paul F. Becher[2]

[1]*Center for Nanophase Materials Sciences, Oak Ridge National Laboratory, Oak Ridge, Tennessee 37831, USA*
[2]*Materials Science and Technology Division, Oak Ridge National Laboratory, Oak Ridge, Tennessee 37831, USA*
[3]*Center for Materials Processing, University of Tennessee, Knoxville, Tennessee 37996-0750, USA*

(Received 26 February 2008; accepted 4 April 2008; published online 25 April 2008)

Electron beam irradiation during scanning transmission electron microscopy has been used to probe the relative abundance and stabilities of gadolinium adsorption sites in polycrystalline silicon nitride ceramics. Site-specific binding strengths in the interface plane between β-Si_3N_4 grains and the adjacent amorphous triple pockets were found to be consistent with theoretical predictions. Decreasing stability was found for Gd within partially ordered planes further from the interface. Atomic level characterization such as that reported here provides detailed insights that will allow one to tailor new functional ceramic microstructures with improved macroscopic mechanical properties. © *2008 American Institute of Physics*. [DOI: 10.1063/1.2917566]

The segregation and adsorption behaviors of rare earth (RE) sintering aids and the resulting crystalline/amorphous interfacial configurations[1–10] critically determine the microstructural evolution of β-Si_3N_4 ceramics. The macroscopic mechanical properties[11–16] of these structural ceramics depend on how strongly RE dopants bind at specific sites, for which until now, no experimental probe has been available. We report the measurement of site-specific binding strengths of Gd atoms segregated to interfaces between crystalline grains and amorphous triple pockets containing glass phases. Atomic and electronic structures at the crystalline/amorphous interfaces were studied by using aberration-corrected scanning transmission electron microscopy[1] (STEM) with single atom sensitivity. A new form of *in situ* STEM was used to assess local binding strength at specific adsorption sites.

Recently, numerous studies have reported about the segregation behavior of various RE atom configurations at β-Si_3N_4 grain boundaries and triple pockets,[2–7,17] including ordered structures extending one or two layers into the glassy phase.[5,7] The presence or absence of RE segregants at specific sites has generally been correlated with theoretical predictions of differential binding energies.[17] In this paper, we show a far more stringent test for theoretical predictions. A time series of atomic-resolution high angle annular dark field (HAADF) STEM images was taken as a probe of the relative stability of *all* observed segregation sites within each layer, i.e., in both interfacial sites and parallel planes extending into the glass phase. At least three ordered layers of Gd atoms lying parallel to the prism plane surface of β-Si_3N_4 grains are observed and examined. The experimental imaging data consistently reproduce theoretical predictions of relative stabilities associated with each layer. In addition, we show that the environment of the Gd atoms is depleted in oxygen. Thus, atomic scale information is provided about the chemical environment and RE binding energies, and these are key requirements for predicting mechanical behavior from first principles.

Figure 1(a) shows a high HAADF image of a grain/triple pocket interface in Gd-doped Si_3N_4. Noise is suppressed by a smoothing (averaging) process.[18] Bright spotlike contrasts along the interface reveal Gd atoms segregated to two inequivalent adsorption sites *A* and *B*, hence, forming a continuous layer (i). From their locations relative to the underlying nitride lattice, we deduce that the Gd atoms are bonded to N atoms in the Si_3N_4 interface plane. One can also observe an ordering of Gd atoms in a second (ii) and a third (iii) layer parallel to the interface extending into the *amorphous* pocket, which is similar to earlier reports.[5,7] The image intensity for the layers decreases from layers (i) though (iii) due to the coupled effect of a decreasing number of RE atoms and an increasing structural disorder that reduces electron channeling. The distances between layers (i) and (ii) and

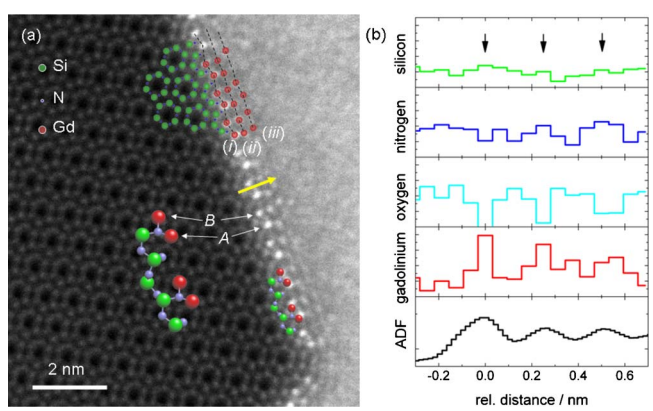

FIG. 1. (Color online) (a) HAADF image of the interface between a Si_3N_4 grain and an adjacent triple pocket containing a Si–Gd–O–N glass. The direction of the electron beam is parallel to the [0001] zone axis in β-Si_3N_4. Three distinct layers of segregated Gd atoms extend into the glassy phase. The ball and stick model in the inset represents the adsorption sites *A* and *B* observed in layer (i). Integrated absorption edge EELS intensities along the yellow arrow are plotted in (b) together with HAADF intensities extracted from (a).

[a)]Electronic mail: benthem@ornl.gov.

 © 2008 American Institute of Physics
Downloaded 23 Feb 2009 to 160.91.159.246. Redistribution subject to AIP license or copyright; see http://apl.aip.org/apl/copyright.jsp

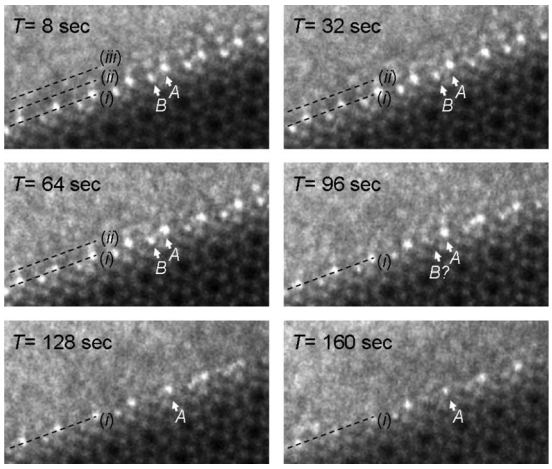

FIG. 2. Six HAADF images extracted from a 21 image time series (Ref. 20). The micrographs have been smoothed to reduce noise (Ref. 18). The first image ($T=8$ s) corresponds to Fig. 1(a), and frames acquired thereafter reveal increasing beam damage effects through the consecutive disappearance of the layers labeled (iii) and (ii), and the subsequent removal of Gd atoms from sites labeled *B* while atoms at the more stable sites *A* remain unchanged.

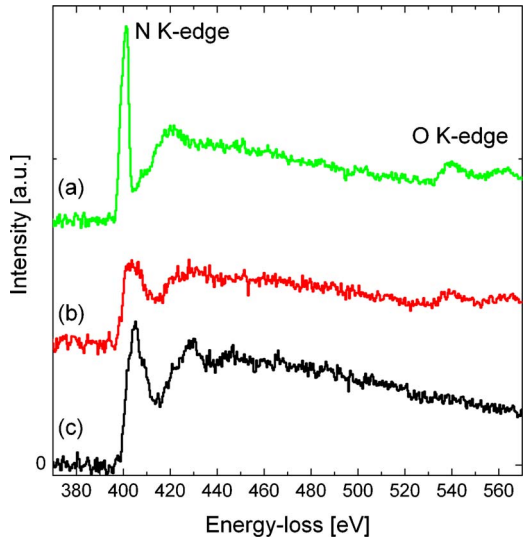

FIG. 3. (Color online) Electron energy-loss near-edge structures of the N *K*- and O *K*-absorption edges recorded from an area (a) within the triple pocket, (b) close to the interface, and (c) inside the Si_3N_4 grain.

layers (ii) and (iii) are 0.25 ± 0.05 nm each, respectively.

To confirm the formation of three ordered layers of Gd atoms, electron energy-loss spectroscopy (EELS) measurements of the Si $L_{2,3}$, Gd $N_{4,5}$, N *K*, and the O *K* absorption edges were performed as line scans across the interface. Figure 1(b) shows the integrated EELS signals for the acquired adsorption edges after background subtraction.[19] Edge intensities were integrated over an interval of 30 eV above the corresponding onset. The Gd signal clearly exhibits three maxima, separated by about 0.25 nm, which are each spatially correlated with one of the three layers observed in Fig. 1(a). For comparison, an ADF intensity line profile is plotted in the bottom panel. Within the experimental error bars, the Si and N signals remain unchanged across the interface. In accord with earlier results by Shibata *et al.*,[7] the oxygen intensity exhibits local minima where the Gd signal peaks. The agreement of ADF imaging and EELS signals prove the formation of at least three ordered layers of Gd atoms, which result from segregation to the grain/triple pocket interface. Hence, a high degree of structural ordering at the previously assumed abrupt crystalline/amorphous interface is apparent and confirmed by two independent experimental techniques. The signal-to-noise ratio for both the ADF image intensity in Fig. 1(a) and the EELS signal in Fig. 1(b) decreases with increasing relative distance due to less structural ordering from layer (i) to layer (iii). This indicates a gradual structural transition from the crystalline Si_3N_4 grains to the fully amorphous triple pocket.

Figure 2 contains six frames taken from a time series of images recorded from the same area displayed in Fig. 1(a). After illuminating the sample with the electron beam for 32 s, the outermost layer (iii) of Gd atoms is no longer visible due to the onset of electron beam damage inside the triple pocket. After an additional 32 s, most of the layer (ii) can also no longer be identified. Adsorption sites in layer (i), i.e., closest to the prismatic interface plane, closely coincide with calculated sites *A* and *B* and show little reduction of Gd intensity until $T=96$ s. Thereafter, a lower intensity from sites labeled *B* indicates a decreasing population of Gd atoms at these weaker binding sites, with no observable change at the higher populated (more strongly bound) adsorption sites labeled *A*. After $T=160$ s, a bright contrast in the HAADF image remains only on adsorption sites *A*, while the bright contrasts at positions B have completely vanished.[20]

The decay in HAADF image intensity at the grain/triple pocket interface is due to atom displacement and, thus, local disordering induced by so-called knock-on processes.[21] The basic mechanism originates from a direct impact of the fast beam electrons with the atomic nuclei. The preferential atom displacement mechanism directly shows that the *A* sites are more resistant to damage than the *B* sites, which is consistent with their larger adsorption energy for Gd atoms and preferential population of *A* sites. The interpretation of these observations straightforwardly follows from the calculated relative energies of Gd–N bonding in different configurations. The formation of locally ordered Gd–N structures within the triple pocket is increasingly hindered as the separation from the grain surface increases, since the template influence of the grain surface decreases relative to disordering effects of the surrounding glass. Hence, fewer Gd atoms form such local Gd–N structures as they fall farther into the glassy pocket. Gd image intensities rapidly decrease as the Gd atoms move away from ordered positions when neighboring N atoms are displaced by the electron beam. The same mechanism determines the eventual loss of the *B*-type Gd intensities from Gd adsorbed at the prism plane. The interfacial N bonds are stronger and thus endure longer than those in the glass. Once an interfacial Gd–N bond breaks, the more weakly bound *B*-type Gd atom displaces more than the *A*-type. However, the observed decrease in *B*-type intensities is also correlated with the lower population of the weaker *B* sites.

Figure 3 shows energy-loss spectra recorded from three different areas: within the amorphous triple pocket [Fig. 3(a)], close to the interface [Fig. 3(b)], and inside the β-Si_3N_4 grain far away from the interface region [Fig. 3(c)]. The Si_3N_4 grain [Fig. 3(c)] shows a typical EELS line shape for the N *K* edge and no evidence for any oxygen signal. In this area, the signal did not show any change over extended periods of electron beam irradiation. Inside the triple pocket but close to the interface [Fig. 3(b)], the EELS data exhibit a

Downloaded 23 Feb 2009 to 160.91.159.246. Redistribution subject to AIP license or copyright; see http://apl.aip.org/apl/copyright.jsp

less intense N *K*-edge signal and clear evidence for the presence of oxygen. When the electron beam is moved further into the triple pocket, indications of beam damage become immediately evident by the formation of a sharp spectral feature at the onset of the N *K* edge [Fig. 3(a)], representing the formation of molecular N_2 leaving the sample.[22,23] This spectral feature dramatically increases in intensity with increasing illumination times. At the same time, the integrated intensity underneath the original N *K* edge gradually decreases, while the O *K*-edge intensity remains unchanged. Thus, we conclude that the Gd atom displacement in the adjacent layers discussed above is due to electron beam induced dislodging of nitrogen atoms from the glass, while oxygen atoms are not affected. Upon electron beam irradiation, the observed effects immediately occur inside the volume of the glassy phases and slightly delayed at the grain/triple pocket interface. We attribute this observation to the more ordered structure and therefore, higher atom density (i.e., stronger binding), close to the interface. The population of specific sites, in turn, reflects the trend in RE adsorbate binding energies of the different sites. By careful control of the beam current densities and, hence, the rate of energy transfer from the beam electrons to the anion nuclei, local RE populations and, thus, relative binding energies, can be *imaged* in a qualitative sense.

Local binding energies for Gd atoms on principal adsorption sites *A* and *B* [Fig. 1(a)] were calculated using density functional theory by using the full potential partial wave self-consistent field atomic cluster approach.[24] Calculated binding energies were calibrated to a local energy maximum on the potential energy surface for displacements of the Gd atom along the [0001] direction. The calculated binding energy results for sites *A* and *B* are 4.54 and 4.01 eV, respectively. The 0.53 eV greater value for site *A* than that for site *B* confirms that Gd atoms at site *A* are more strongly bound and, therefore, (a) populate *A* sites more than *B* sites and (b) are more stable under electron beam irradiation. The experimental observations outlined above are consistent and in qualitative agreement with these results.

In the present study, the experimental confirmation of theoretically predicted differences in local population densities and binding energies for Gd atoms segregated to crystalline/amorphous interfaces in Si_3N_4 using aberration-corrected STEM was reported. Structural ordering of the Gd–N network close to the interface is altered by electron beam impact. However, the time evolution of electron beam damage, which is usually considered undesirable and detrimental, can be used as an analytical tool for probing the local binding strengths of specific atomic sites when exposure time is simultaneously monitored. A detailed understanding of the local bonding characteristics and, hence, the structural ordering will help to formulate design strategies for structural and functional ceramics with specific interface features and consequently predictable macroscopic properties.

We dedicate this paper to Dr. G. S. Painter, who unexpectedly passed away while the manuscript was being reviewed. Research sponsored by U.S. DOE, Division of Materials Sciences and Engineering. K.v.B. was also supported by the Division of Scientific User Facilities (manuscript preparation), by appointment to the ORNL Postdoctoral Research Program administered jointly by ORNL and ORISE, and a Feodor-Lynen scholarship of the Alexander von Humboldt Foundation.

[1] N. Shibata, S. J. Pennycook, T. R. Gosnell, G. S. Painter, W. A. Shelton, and P. F. Becher, Nature (London) **428**, 730 (2004).
[2] A. Ziegler, J. C. Idrobo, M. K. Cinibulk, C. Kisielowski, N. D. Browning, and R. O. Ritchie, Science **306**, 1768 (2004).
[3] A. Ziegler, J. C. Idrobo, M. K. Cinibulk, C. Kisielowski, N. D. Browning, and R. O. Ritchie, Appl. Phys. Lett. **88**, 041919 (2006).
[4] C. Dwyer, A. Ziegler, N. Shibata, G. B. Winkelman, R. L. Satet, M. J. Hoffmann, M. K. Cinibulk, P. F. Becher, G. S. Painter, N. D. Browning, D. J. H. Cockayne, R. O. Ritchie, and S. J. Pennycook, J. Mater. Sci. **41**, 4405 (2006).
[5] G. B. Winkelmann, C. Dwyer, C. Marsh, T. S. Hudson, D. Nguyen-Manh, M. Doblinger, and D. J. H. Cockayne, Mater. Sci. Eng., A **422**, 77 (2006).
[6] G. B. Winkelmann, C. Dwyer, T. S. Hudson, D. Nguyen-Manh, M. Doblinger, R. L. Satet, M. J. Hoffmann, and D. J. H. Cockayne, Appl. Phys. Lett. **87**, 061911 (2005).
[7] N. Shibata, G. S. Painter, P. F. Becher, and S. J. Pennycook, Appl. Phys. Lett. **89**, 051908 (2006).
[8] M. J. Hoffmann and G. Petzow, Pure Appl. Chem. **66**, 1807 (1994).
[9] A. Subramaniam, C. T. Koch, R. M. Cannon, and M. Rühle, Mater. Sci. Eng., A **422**, 3 (2006).
[10] K. van Benthem, G. Tan, L. K. Denoyer, R. H. French, and M. Rühle, Phys. Rev. Lett. **93**, 227201 (2004).
[11] P. F. Becher, G. S. Painter, E. Y. Sun, C. H. Hsueh, and M. J. Lance, Acta Mater. **48**, 4493 (2000).
[12] P. F. Becher, E. Y. Sun, K. P. Plucknett, K. B. Alexander, C. H. Hsueh, H. T. Lin, S. B. Waters, C. G. Westmoreland, E. S. Kang, K. Hirao, and M. E. Brito, J. Am. Ceram. Soc. **81**, 2821 (1998).
[13] E. Y. Sun, P. F. Becher, K. P. Plucknett, C. H. Hsueh, K. B. Alexander, S. B. Waters, K. Hirao, and M. E. Brito, J. Am. Ceram. Soc. **81**, 2831 (1998).
[14] E. Y. Sun, P. F. Becher, C. H. Hsueh, G. S. Painter, S. B. Waters, S. L. Hwang, and M. J. Hoffmann, Acta Mater. **47**, 2777 (1999).
[15] P. F. Becher, G. S. Painter, M. J. Lance, S. Ii, and Y. Ikuhara, J. Am. Ceram. Soc. **88**, 1222 (2005).
[16] R. L. Satet and M. J. Hoffmann, J. Am. Ceram. Soc. **88**, 2485 (2005).
[17] G. S. Painter, P. F. Becher, W. A. Shelton, R. L. Satet, and M. J. Hoffmann, Phys. Rev. B **70**, 144108 (2004).
[18] Smoothing was carried out by using the DIGITALMICROGRAPH software package provided by Gatan, Inc. (www.gatan.com).
[19] R. F. Egerton, *Electron Energy-Loss Spectroscopy in the Electron Microscope*, 2nd ed. (Plenum, New York, 1996).
[20] See EPAPS Document No. E-APPLAB-92-065817 for a video clip of the time evolution of electron beam damage effects illustrating differences in the binding energies of the different adsorption sites of Gd. For more information on EPAPS, see http://www.aip.org/pubservs/epaps.html.
[21] L. Reimer, *Transmission Electron Microscopy* (Springer, Heidelberg, 1997).
[22] N. J. Zaluzec and J. F. Mansfield, *Proceedings of 44th Annual Meeting of the Microscopy Society of America*, 1986, p. 708.
[23] K. A. Mkhoyan and J. Silcox, Appl. Phys. Lett. **82**, 859 (2003).
[24] F. W. Averill and G. S. Painter, Phys. Rev. B **50**, 7262 (1994).

Downloaded 23 Feb 2009 to 160.91.159.246. Redistribution subject to AIP license or copyright; see http://apl.aip.org/apl/copyright.jsp